

Neutron Charge Radius Deduced from Interferometric Bragg Reflection Technique

J.-M. Sparenberg* and H. Leeb

*Atominstitut der Österreichischen Universitäten, Technische Universität Wien,
Wiedner Hauptstraße 8-10, A-1040 Vienna, Austria*

(Dated: November 20, 2018)

Abstract

The possibility of the determination of the neutron mean square charge radius from high-precision thermal-neutron measurements of the nuclear scattering length and of the scattering amplitudes of Bragg reflections is considered. Making use of the same interferometric technique as Shull in 1968, the scattering amplitudes of about eight higher-order Bragg reflections in silicon could be measured without contamination problem. This would provide a value of the neutron charge radius as precise as the disagreeing Argonne-Garching and Dubna values, as well as a Debye-Waller factor of silicon ten times more precise than presently available.

PACS numbers: 03.75.Be, 03.75.Dg, 13.60.Fz, 14.20.Dh

arXiv:quant-ph/0201059v1 15 Jan 2002

* on leave from Université Libre de Bruxelles, PNTPM-CP 229, Campus de la Plaine, B-1050 Brussels, Belgium.

The so-called mean square charge radius of the neutron $\langle r_n^2 \rangle$ is an important structure constant which reflects the internal charge structure of the neutron. In terms of the generally used form factors, $\langle r_n^2 \rangle$ is related to the derivative of the Sachs form factor G_E^n at vanishing transferred momentum Q ,

$$\langle r_n^2 \rangle = -\frac{1}{6} \left. \frac{dG_E^n}{dQ^2} \right|_{Q=0}. \quad (1)$$

Low-energy neutron-atom scattering experiments have been found useful [1, 2] to determine $\langle r_n^2 \rangle$ via high-precision measurements of the neutron-electron scattering length b_{ne} ,

$$b_{ne} = \frac{1}{3} \frac{\alpha m_n c^2}{\hbar c} \langle r_n^2 \rangle, \quad (2)$$

where m_n is the mass of the neutron. Because of the fundamental importance of these quantities for our understanding of the nucleon many ambitious experiments have been performed in the last decades (see e.g. [3] and references therein).

Despite these efforts the determination of b_{ne} is still unsatisfactory because there exist two sets of results which differ more than three standard deviations from each other. In this paper we propose an independent method based on high-precision measurements of neutron Bragg reflections on silicon. Assuming for all higher-order reflections a precision similar to that achieved by Shull [4] one can solve the discrepancy in the values of b_{ne} .

In a first theoretical estimate, b_{ne} is expected to be given by the Foldy scattering length [5],

$$b_{ne}^{\text{theory}} = -1.467971(4) \times 10^{-3} \text{ fm}, \quad (3)$$

corresponding to the well-known value of the anomalous magnetic moment of the neutron [6]. The actual b_{ne} value can be deduced from low-energy neutron-atom scattering, for which the “scattering length” reads [1]

$$\begin{aligned} b(Q) &= b_{\text{nuclear}} \underbrace{-b_{ne}Z[1-f(Q)]}_{\text{electrostatic}} \quad (4) \\ &= b_{\text{nucleus}} + \underbrace{b_{ne}Zf(Q)}_{\text{electrons}}, \quad (5) \end{aligned}$$

where b_{nuclear} is the nuclear-interaction scattering length, b_{nucleus} is the neutron-nucleus scattering length (nuclear and electrostatic interactions), Z is the atomic number and $f(Q)$ is the atomic form factor normalized to the forward direction: $f(0) = 1$. In Eq. (4), the

Q -dependent electrostatic term is typically three orders of magnitude smaller than the constant nuclear term, hence it is reasonable to speak of “scattering length” despite the Q dependence. To get a sufficiently high sensitivity to this term scattering processes at $Q \neq 0$ (hence $0 < f(Q) < 1$) and high Z should be chosen.

The best experimental values of b_{ne} (see e.g. Table I in [7]) can be grouped into two sets. Those deduced from thermal-neutron angular scattering on noble gases [8] and from thermal- and epithermal-neutron transmission on liquid lead and bismuth [3, 9] agree on the value $b_{\text{ne}} = -1.31(3) \times 10^{-3}$ fm (Argonne-Garching). The second set of b_{ne} values obtained from another transmission experiment on Bi [10] and a measurement of thermal-neutron Bragg reflections on tungsten monocrystals [11] are centered about $b_{\text{ne}} = -1.59(4) \times 10^{-3}$ fm (Dubna). There is a clear discrepancy because the b_{ne} values of the two sets differ more than three standard deviations from each other. In addition they differ about 10% from $b_{\text{ne}}^{\text{theory}}$, one being smaller than $b_{\text{ne}}^{\text{theory}}$, the other larger. While the difference in the b_{ne} values obtained from the Bi-transmission experiments [3, 10] is well understood [7, 9, 12], the Bragg-reflection method of Ref. [11] has never been revisited. In the latter experiment, the value of b_{ne} is extracted from the slope of $b(Q)$ as a function of $1 - f(Q)$ [see Eq. (4)]. The fitted data are the forward value b_{nuclear} , obtained from a Christiansen-filter experiment, and the values for eight Bragg reflections $b(Q_{hkl})$. The transferred momentum Q_{hkl} reads

$$Q_{hkl}/4\pi = \sqrt{h^2 + k^2 + l^2}/2a_0 = \sin \theta_{hkl}/\lambda, \quad (6)$$

where (hkl) are the Miller indices, a_0 is the side of the conventional cubic unit cell, θ_{hkl} is the Bragg angle and λ is the neutron wavelength.

For two different crystals, two very different values of b_{ne} were obtained in Ref. [11]: i.e., $b_{\text{ne}} = -1.06$ and -2.2×10^{-3} fm, which led the authors to postulate the existence of an additional scattering process. We rather consider that this discrepancy reveals the systematic uncertainty of the experiment, where $b(Q_{hkl})$ is deduced from an integral-intensity measurement of the Bragg peak. This systematic uncertainty has probably been underestimated in Ref. [11] for different reasons: (i) extinction is neglected, (ii) the uncertainty on the temperature factor (which is shown below to be of crucial importance) is neglected. Consequently, the accuracies obtained for $b(Q_{hkl})$ (typically 0.01 fm) seem unrealistic as compared with accuracies generally obtained by this kind of measurement (typically 0.1 fm) [13]. A hint to our conjecture is also given by the strong disagreement between other results

[14] obtained *inter alia* with an integral-intensity measurement on monocrystals, and the Christiansen-filter results of Ref. [15] for W isotopes.

Let us now consider the method proposed by Shull in Ref. [4], which also aims at measuring $b(Q_{hkl})$ for Bragg reflections on monocrystals. We refer to Ref. [4] for details about the experimental setup. A collimated full-spectrum incident beam is Bragg reflected on a monocrystal blade (typical thickness $t = 1$ cm) in Laue transmission geometry. The wavelength selection is made through the Bragg condition (6), the crystal and the detector being moved simultaneously to form angles θ and 2θ respectively with the incident-beam direction. As shown in the dynamical theory of Bragg reflection for neutrons [6, 13], the reflected beam inside the crystal consists of two coherent waves, the so-called *Pendellösung* (pendulum solutions), interfering with each other and generating Pendellösung oscillations. An entrance and a scanning gadolinium slits (width 0.13 mm) are placed on both faces of the crystal to extract these fringes. Making use of the symmetry of the interference pattern a very precise alignment of the scanning slit with respect to the entrance slit is possible. The intensity at the center of the interference pattern is then measured as a function of the wavelength and compared with the theoretical expression. This expression may be obtained either by the Kato spherical-wave dynamical theory [16] or by solving the Takagi-Taupin equations [6]. For a perfectly-flat crystal and with infinitely-narrow slits, this intensity reads

$$I_{hkl}(\lambda) \propto I_0(\lambda)\lambda^2|F_{hkl}|^2 J_0^2 \left(\frac{t|F_{hkl}|}{a_0^3 \cos \theta_{hkl}(\lambda)} \lambda \right), \quad (7)$$

where I_0 is the incident intensity, J_0 is a Bessel function and $|F_{hkl}|$ is the unit-cell structure factor of the crystal. This expression has to be slightly modified to take into account the finite curvature of the crystal, which adds the curvature radius R (typically 20 km) as a parameter to be fitted to the data, and to take into account the finite opening of the slits [16]. Typically, forty fringes are observed for neutrons ranging the full spectrum of a thermal reactor. The structure factor can then be deduced with high precision from the period of these fringes. Shull's method is thus in essence an interferometric method, which explains why it provides very high accuracies (contrary to the integral-intensity method).

For a diamond-structure crystal like silicon, the unit cell consists of four elementary cells with two atoms. The corresponding structure factor reads [13]

$$F_{hkl} = 4 \times \left(1 + i^{h+k+l} \right) \times b_{\text{meas}}(Q_{hkl}), \quad (8)$$

where $b_{\text{meas}}(Q)$ is related to $b(Q)$ through the Debye-Waller temperature factor [13]

$$b_{\text{meas}}(Q) = b(Q) \times \exp \left[-B(Q/4\pi)^2 \right]. \quad (9)$$

To get a precise $b(Q_{hkl})$ value, as needed to estimate b_{ne} , one needs precise values of both the structure factor F_{hkl} and the temperature parameter B . For instance, for the (111) reflection on Si ($Z = 14$, $a_0 = 5.43072 \text{ \AA}$), Shull's method provides [16] $b_{\text{meas}}(Q_{111}) = 4.1053(8) \text{ fm}$. Using the Debye-Waller factor obtained by measuring X-ray Pendellösung fringes at room temperature [17]

$$B = 0.4613(27) \text{ \AA}^2, \quad (10)$$

one gets

$$b(Q_{111}) = 4.1538(11) \text{ fm}, \quad (11)$$

where three additional units in the error are due to the error on B . Equation (9) shows that this additional uncertainty increases exponentially with Q^2 (see Fig. 1).

Following the approach of Ref. [16], we can deduce b_{nuclear} from value (11) with Eq. (4), using the Argonne-Garching b_{ne} and the atomic form factor [18]: $f(Q_{111}) = 0.7526$ (a precise value of $f(Q)$ is actually not required [1]). This yields $b_{\text{nuclear}} = 4.1495(11) \text{ fm}$ (which slightly differs from the value of Ref. [16] because of the more recent temperature factor), in agreement with the more precise value obtained recently by non-dispersive-sweep neutron interferometry [19]

$$b_{\text{nuclear}} = 4.1507(2) \text{ fm}. \quad (12)$$

Conversely, b_{ne} can be deduced from values (11) and (12) with Eq. (4), which provides (see Fig. 1)

$$b_{\text{ne}}^{\text{Si}} = -0.89(32) \times 10^{-3} \text{ fm}. \quad (13)$$

This value agrees with the Argonne-Garching value but does not exclude the Dubna value (see Fig. 2). The same method applied to germanium (diamond structure with $a_0 = 5.6575 \text{ \AA}$) using $b_{\text{nuclear}} = 8.1929(17) \text{ fm}$ [20], $b_{\text{meas}}(Q_{111}) = 8.0829(15) \text{ fm}$ [21], $B = 0.57(1) \text{ \AA}^2$ [22] and $f(Q_{111}) = 0.8542$ [18], leads to the value $b_{\text{ne}}^{\text{Ge}} = 0.28(83) \times 10^{-3} \text{ fm}$. Although measurements on Ge ($Z=32$) could in principle lead to a value of b_{ne} two times more precise

than on Si ($Z = 14$), this advantage is compensated by the two-times-larger scattering length, which implies a two-times-larger absolute error on $b(Q_{hkl})$, the relative accuracy of Shull's method being 0.02% in both cases. Moreover, no b_{nuclear} value for Ge of comparable precision to (12) is available at present. Hence we only consider Si in the following.

In Fig. 1, values (11) and (12) are represented as a function of $1 - f(Q)$. It is seen that the (111) reflection is not the optimal choice to calculate the slope of the line since it is close to the origin. Higher-order reflections are more appropriate, as shown by the simulated data. The error bars of these simulated points are calculated with the error $\sigma_B = 0.0027 \text{ \AA}^2$ on the temperature factor (10) only, assuming an ideal experiment with an infinite accuracy on b_{meas} . With such large uncertainties, there is no hope to reach a high precision on b_{ne} , in particular to distinguish between the Argonne-Garching (solid line in Fig. 1) and Dubna (broken line) values. However, if enough (at least two) reflections are measured, *both* B and b_{ne} could be deduced from the data. The precision of the extracted B and b_{ne} can be improved by increasing the number of reflections.

Let us now determine the possibly-observable reflections. A diamond-structure crystal has a face-centered cubic lattice, which implies that all Miller indices have to be either even or odd [13]. Moreover, for a diamond structure, the structure factor (8) leads to three types of reflections: (i) forbidden when $h + k + l = 2 + 4n$, where n is natural, (ii) weak when $h + k + l$ is odd, (iii) strong when $h + k + l = 4 + 4n$. A thermal-neutron beam has typically a maximum flux for $\lambda = 1.2 \text{ \AA}$ and the accessible angular range of the setup is assumed to be $0 \leq 2\theta \leq 110^\circ$. These conditions combined with Eq. (6) imply that sixteen reflections between (111) and (642) could be measured with reasonable intensities for Si. However, if the incident beam has a typical full spectrum $0.8 \leq \lambda \leq 2.5 \text{ \AA}$, contamination has to be taken into account. For instance, while the (111) reflection is pure for $15 \leq 2\theta \leq 45^\circ$ thanks to the absence of the (222) reflection which is forbidden (hence the result of Refs. [4, 16]), (333) and (444) would be measured on $45 \leq 2\theta \leq 110^\circ$ and $61 \leq 2\theta \leq 110^\circ$ respectively. This mixing implies that the reflected intensity would not be described by Eq. (7) and that no structure factor could easily be extracted. Among the sixteen considered reflections, seven could be contaminated. The remaining nine reflections are listed in Table I. Three crystal blades would suffice to measure them all [for instance, a crystal blade cut parallel to the (220) planes could be used to measure the (111), (422), (511), (533), (711) and (551) reflections]. Among these reflections, three are strong (underlined in Table I); the intensities

range between 0.7 and 1.7 times the intensity of the already-measured (111) weak reflection. Finally, Eq. (7) allows to estimate the number of fringes which would be measured for each of them. For instance, 44 fringes would be observed for the (711) reflection if $t = 1$ cm.

These considerations show that these higher reflections should not be more complicated to measure than the (111) reflection already measured in Refs. [4, 16]. Hence, we can reasonably assume that the precision on b_{meas} would be equal to that of Ref. [16]: 0.0008 \AA . With this assumption, the attainable precision for B and b_{ne} can be estimated. For B , we apply the approximate linear relation [Eqs. (4) and (9)]

$$\ln b_{\text{meas}}(Q) \approx \ln b_{\text{nuclear}} - B(Q/4\pi)^2, \quad (14)$$

while for b_{ne} we use Eq. (4). The uncertainty of a linear-fit slope can be calculated from the abscissas of the experimental points and from their errors [23]. Measuring the three strong reflections would give

$$\sigma_B = 0.00040 \text{ \AA}^2, \sigma_{b_{\text{ne}}} = 0.11 \times 10^{-3} \text{ fm}, \quad (15)$$

while with the eight new reflections of Table I, one gets

$$\sigma_B = 0.00027 \text{ \AA}^2, \sigma_{b_{\text{ne}}} = 0.06 \times 10^{-3} \text{ fm}. \quad (16)$$

The temperature factor would be ten times more precise than the most precise value (10) and the b_{ne} value would be nearly as precise as the Argonne-Garching and Dubna values (see Fig. 2). Since the present method is similar to the Dubna method on W, such a new result would certainly be of great help to decide the b_{ne} discrepancy.

In conclusion, the measurement of Pendellösung fringes in Bragg reflections is a very powerful technique. This is known for X-rays [17, 24] but generally ignored for neutrons. By confirming Shull's pioneer conclusion [4]

“... the high sensitivity of the fringe positions ... can be exploited ... [for] example ... in assessing the neutron-electron interaction strength...”

the present work opens new prospects for the field of *Neutron Pendellösung Interferometry*.

We acknowledge useful discussions with H. Rauch, H. Kaiser and E. Jericha. J.-M. S. is supported by the European TMR program ERB-FMRX-CT96-0057 on perfect-crystal neutron optics and by the National Fund for Scientific Research (Belgium). He thanks the members of the Atominstitut for their hospitality.

-
- [1] V. F. Sears, Phys. Rep. **141**, 281 (1986).
- [2] Y. A. Alexandrov, *Fundamental Properties of the Neutron*, no. 6 in Oxford Series on Neutron Scattering in Condensed Matter (Oxford University, New York, 1992).
- [3] S. Kopecky, J. A. Harvey, N. W. Hill, M. Krenn, M. Pernicka, P. Riehs, and S. Steiner, Phys. Rev. C **56**, 2229 (1997).
- [4] C. G. Shull, Phys. Rev. Lett. **21**, 1585 (1968).
- [5] L. L. Foldy, Rev. Mod. Phys. **30**, 471 (1958).
- [6] H. Rauch and S. A. Werner, *Neutron Interferometry. Lessons in Experimental Quantum Mechanics*, no. 12 in Oxford Series on Neutron Scattering in Condensed Matter (Oxford University, New York, 2000).
- [7] H. Leeb and C. Teichtmeister, Phys. Rev. C **48**, 1719 (1993).
- [8] V. E. Khron and G. R. Ringo, Phys. Rev. D **8**, 1305 (1973).
- [9] L. Koester, W. Waschkowski, L. V. Mitsyna, G. S. Samosvat, P. Prokofjevs, and J. Lamberg, Phys. Rev. C **51**, 3363 (1995).
- [10] Y. A. Alexandrov, M. Vrana, G. J. Manrique, T. A. Machekhina, and L. N. Sedlakova, Sov. J. Nucl. Phys. **44**, 1384 (1986).
- [11] Y. A. Alexandrov, T. A. Machekhina, L. N. Sedlakova, and L. E. Fykin, Sov. J. Nucl. Phys. **20**, 623 (1975).
- [12] Y. A. Alexandrov, Phys. Rev. C **49**, R2297 (1994).
- [13] V. F. Sears, *Neutron Optics. An introduction to the Theory of Neutron Optical Phenomena and Their Applications*, no. 3 in Oxford Series on Neutron Scattering in Condensed Matter (Oxford University, New York, 1989).
- [14] Y. A. Alexandrov, A. M. Balagurov, E. Malisewski, T. A. Machekhina, L. N. Sedlakova, and A. Holas, Sov. J. Nucl. Phys. **10**, 189 (1970).
- [15] K. Knopf and W. Waschkowski, Z. Naturforsch. **42a**, 909 (1987).
- [16] C. G. Shull and J. A. Oberteuffer, Phys. Rev. Lett. **29**, 871 (1972).
- [17] P. J. E. Aldred and M. Hart, Proc. R. Soc. London A **332**, 223 (1973).
- [18] D. T. Cromer and J. B. Mann, Acta Cryst. **A24**, 321 (1968).
- [19] A. Ioffe, D. L. Jacobson, M. Arif, M. Vrana, S. A. Werner, P. Fischer, G. L. Greene, and

- F. Mezei, Phys. Rev. A **58**, 1475 (1998).
- [20] C. S. Schneider, Acta Cryst. **A 32**, 375 (1976).
- [21] C. G. Shull and W. M. Shaw, Z. Naturforsch. **28 a**, 657 (1973).
- [22] N. M. Butt, J. Bashir, B. T. M. Willis, and G. Heger, Acta Cryst. **A 44**, 396 (1988).
- [23] W. H. Press, B. P. Flannery, S. A. Teukolsky, and W. T. Vetterling, *Numerical Recipes. The Art of Scientific Computing (FORTRAN Version)* (Cambridge University, New York, 1989).
- [24] T. Saka and N. Kato, Acta Cryst. **A42**, 469 (1986).

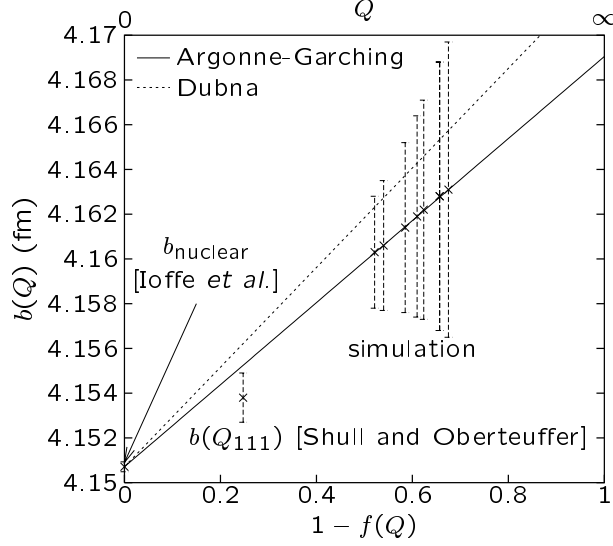


FIG. 1: Experimental b_{nuclear} of Eq. (12) and $b(Q_{111})$ of Eq. (11) compared with the theoretical curves (4) for $b_{\text{nuclear}} = 4.1507$ fm, $b_{\text{ne}} = -1.31$ (Argonne-Garching) and -1.59×10^{-3} fm (Dubna). The simulated points correspond to the reflections of Table I; they are calculated with the Argonne-Garching b_{ne} value, with error bars only due to the uncertainty on the temperature factor (10).

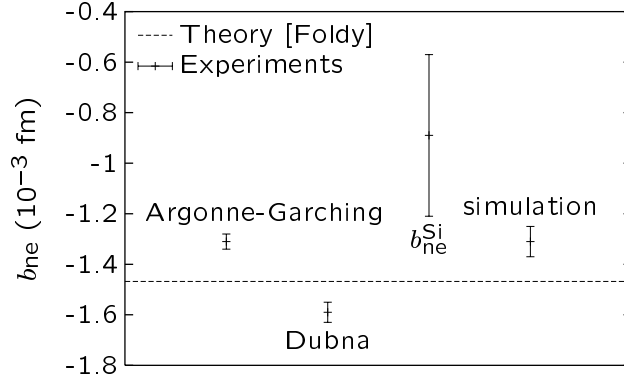


FIG. 2: Comparison of the theoretical b_{ne} value (3) with the Argonne-Garching and Dubna experimental values and with the result (13). The simulated point has the Argonne-Garching value with the error bar of Eq. (16).

TABLE I: Weak and strong (underlined) Bragg reflections which could be measured with a thermal-neutron reactor without contamination problem. (hkl) are the Miller indices, $f(Q_{hkl})$ is the atomic form factor [18], λ the neutron-wavelength interval, 2θ the corresponding angles between the incident and reflected beams. $|F_{hkl}|^2$ is the squared structure factor which provides the reflection intensity through Eq. (8).

(hkl)	$f(Q_{hkl})$	λ (Å)	2θ (°)	$ F_{hkl} ^2$ (Å ²)
(111)	0.7526	0.8-2.5	15-47	540
<u>(422)</u>	0.4788	0.8-1.8	42-110	<u>918</u>
(511)	0.4600	0.8-1.7	45-110	448
(531)	0.4150	0.8-1.5	52-110	421
<u>(620)</u>	0.3902	0.8-1.4	56-110	<u>811</u>
(533)	0.3764	0.8-1.4	58-110	396
(551)	0.3432	0.8-1.2	63-110	372
(711)	0.3432	0.8-1.2	63-110	372
<u>(642)</u>	0.3249	0.8-1.2	67-112	<u>715</u>